CHALMERS
UNIVERSITY OF TECHNOLOGY

Coupled finite element analysis of a partially saturated slope in Norway.

Proceedings 10th NUMGE 2023
10th European Conference on Numerical Methods in Geotechnical Engineering
Zdravkovic L, Kontoe S, Taborda DMG, Tsiampousi A (eds)

https://doi.org/10.53243/NUMGE2023-36

Coupled finite element analysis of a partially saturated slope in Norway

V. Mangraviti[1], V. Capobianco[2], L. Piciullo[2], J. Dijkstra[1]

[1]*Department of Architecture and Civil Engineering, Chalmers University of Technology, Gothenburg, Sweden*
[2]*Norwegian Geotechnical Institute, Oslo, Norway*

ABSTRACT: Climate change induces high variability in environmental loading, such as rainfall patterns, snowing and melting processes, temperature variations. These climatic variables are expected to influence the occurrence of landslides in the upcoming years. Specifically, significant variations in rainfall frequency and intensity would affect the risk posed to structures and linear infrastructures. As a result, more efficient and real-time monitoring techniques and stability analyses will be required. The aim of this study is to couple predictive numerical models with monitoring data for slopes along infrastructures to set-up warning tools to help stakeholders in decision making. The hydro-mechanical response of a well-monitored unsaturated slope, adjacent to a railway line, when subjected to rainfall events is investigated. A numerical Finite Element model has been developed and validated with in-situ measurements. The hypotheses at the base of the modelling, together with the calibration of unsaturated conditions, will be discussed. The results of a fully coupled hydro-mechanical analysis for different rainfall scenarios will be shown.

Keywords: unsaturated soils; rainfall; fully coupled hydro-mechanical analysis; FEM

1 INTRODUCTION

Rainfall-induced shallow landslides are mainly triggered by water infiltration into the soil and may represent a hazard to existing linear infrastructures, with serious societal and economic consequences. Prolonged rainfall provokes a rapid reduction of suction in the uppermost layer of soils with a consequential reduction of shear strength up to failure (Alonso et al., 2003; Salciarini and Tamagnini, 2015). In addition, the reduction of the degree of saturation (S) of the soil significantly affects the infiltration process, as soil permeability strongly decreases with decreasing S. In practice, partially saturated conditions of the superficial layers of the slope are often neglected, both because of the increased complexity of the problem, and because considering a slope in fully saturated condition is on the safe side. However, it is now widely recognized that suction plays an important role in slope stability analyses, particularly when the effect of rainfall on slope deformations is studied.

Nowadays, landslide monitoring and early warning systems are effective tools available to safeguard infrastructures from climate-induced geohazards where structural mitigations measures are not possible. In this study, available field investigation data and laboratory tests were used to create a hydromechanically coupled model of a Norwegian unsaturated slope. Particular attention was given to the unsaturated soil conditions above the water table and to the influence of the rainfall on the deformations of the slope. Recorded pore-water pressures were used to identify the hydrogeological conditions of the slope. The nature of the slope infiltration mechanisms and the complex relationships between the mechanical and the hydraulic response are discussed comparing measurements and calculations of the S.

2 CASE STUDY

The site studied is a 25-30 m high slope in Eidsvoll municipality (Norway), with an inclination reaching ca. 45° near the crest. Two railway lines are located near the toe of the slope, one of those was recently constructed in 2021. In addition, a cultural heritage area, with an old church from the 12th century and its graveyard, is located at the top of the slope, making the realisation of some structural slope stability measures, such as reducing the slope inclination, a non-viable solution. The slope, whose failure may hazardously affect the railway lines, has not exhibited any significant deforma-

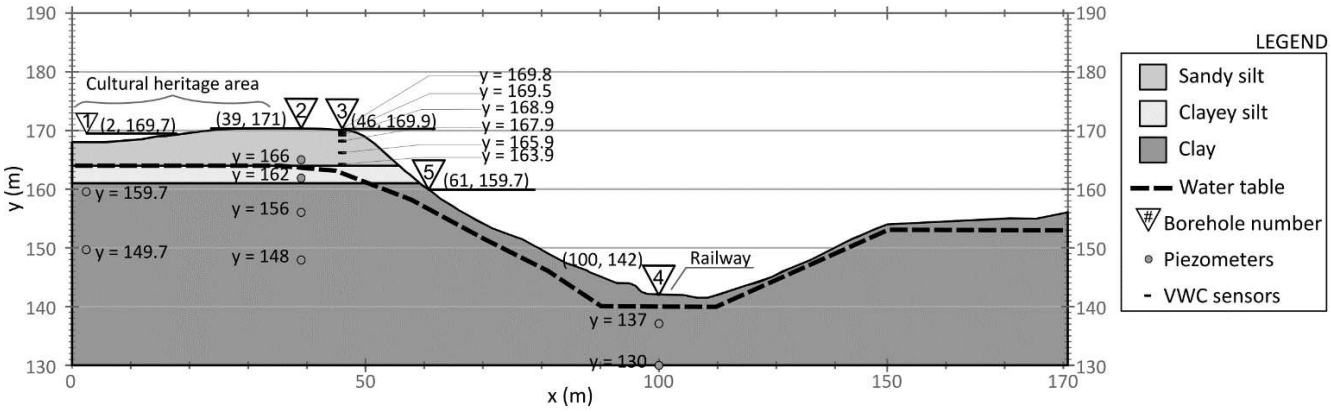

Figure 1. Cross section of slope, soil stratigraphy, water table position and location of the sensors.

tion so far. A nearby slope failure recently occurred during a period of intense precipitation (Heyerdahl et al., 2018), therefore, sensors were installed to monitor hydrological conditions in the studied slope.

Volumetric water content (VWC) and porewater pressure (PWP) sensors were installed in late spring/early summer of 2016 to monitor the hydrological conditions (as described in Heyerdahl et al., 2018). Five boreholes were realised in the studied area, where sensors were installed at different depths (see Figure 1 and Table 1 for more details).

CPTu tests were performed near all the borehole locations and used in this study to define the stratigraphy of the slope. Boreholes 2 and 5 were used to collect samples at different depths for standard lab tests (constant rate of strain, CRS, and undrained triaxial tests with anisotropic consolidation, CK_0U), used to identify the mechanical properties of the soil layers.

The slope has been schematised with three homogeneous layers. From top to bottom: one sandy silt layer of about 6 m, a thinner clayey silt layer (about 3 m thick) and a firm marine clay layer to large depths (Figure 1).

Table 1. Depth of sensors (P = piezometer; VWC = volumetric water content sensor) for each borehole in Figure 1.

Borehole #	Sensor	Depth (m)
1	P	10
		20
2	P	5
		9
		15
		23
3	VWC	0.1
		0.5
		1
		2
		4
		6
4	P	5
		12

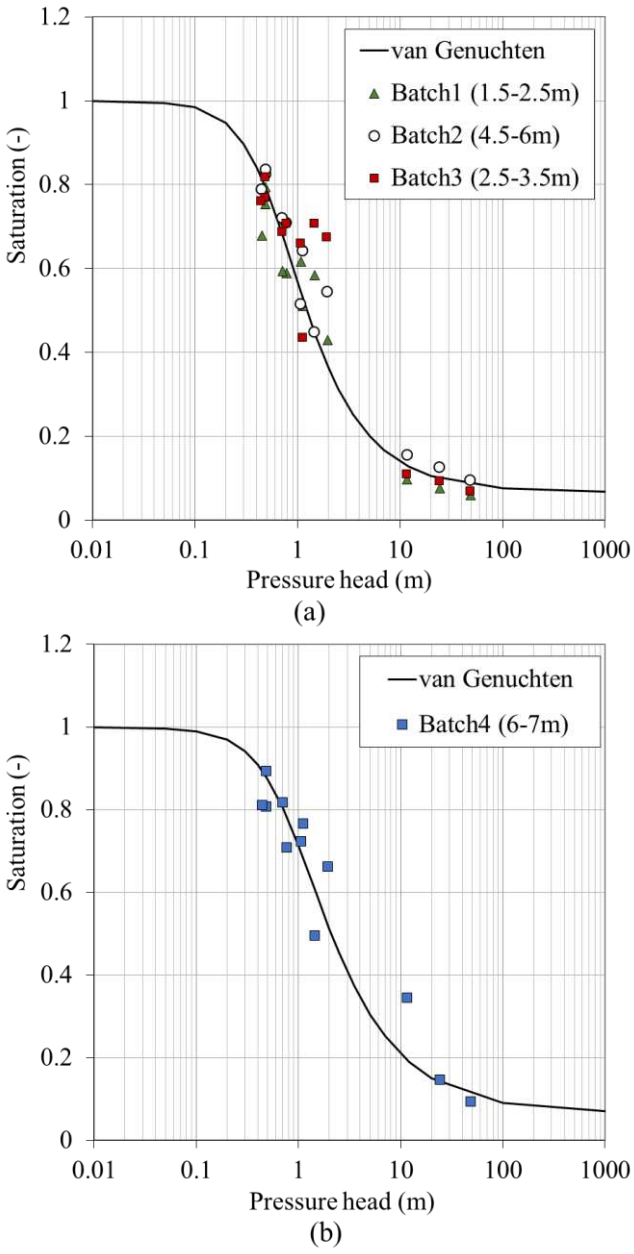

Figure 2 – Soil water retention curves for the drying phase obtained by interpolating the results from pressure plate tests. (a) sandy silt layer, 0 ÷ 6 m depth; (b) clayey silt layer, 6 ÷ 7 m depth.

At the top of the slope, the seasonal average water table level is at about 7 m depth, so that the top layers are partially saturated. The slope is fully saturated at the toe, as stated from field measurements.

To investigate the unsaturated properties of the two layers at the top, pressure plate tests were performed by Heyerdahl et al. (2018). Four different batches were considered between 1.5 and 7 m depth, for the determination of the soil water retention curves (SWRC) for the drying phase in the sandy silt (Figure 2(a)) and clayey silt (Figure 2(b)) layers.

3 FINITE ELEMENT MODEL

In this study, the finite element code Plaxis 2D Ultimate (BentleySystems, 2022) was used to solve the coupled hydromechanical problem at serviceability state level (solving together the hydraulic problem and the equilibrium, see PLAXIS, 2021), under different rainfall scenarios. Stability analyses to evaluate the safety factor, under ultimate limit state conditions, are not the object of this study. Further details on the hydrological back-calculation, and the set-up of an Internet of Things (IoT)- based slope stability analysis and early warning system is discussed in Piciullo et al. (2022).

Different rain and snowmelting data series, measured in the Minnesund station (Eidsvoll area), were considered to study the mechanical response of the slope in terms of both hydraulic response and deformations under rainfall and snow melting.

The domain was discretised in 15230 triangular elements, with 15 nodes each. Each element provides a fourth order interpolation for both displacements and the numerical integration involves twelve Gauss points, as for pore pressures. The spatial discretisation was optimised by reducing the element size where more deformations are expected (close to the surface, where the rain infiltrates).

Normal displacements are fixed on the boundaries. An elastic perfectly plastic constitutive behaviour, with a Mohr-Coulomb (MC) failure criterion was used for the unsaturated layers near the top. A modified Cam-clay (MCC) model was chosen for the over consolidated clay. The parameters of the constitutive models were calibrated on lab test results available at different depths from boreholes 2 and 5 (see

Table 2). Bishop's effective stresses are implemented in the unsaturated analysis.

The unsaturated behaviour was modelled with the van Genuchten model (van Genuchten, 1980), whose parameters were calibrated on the data in Figure 2. In particular, the three-parameter equation implemented by Plaxis relates the saturation (S) to the pressure head (ψ):

$$S = S_{res} + (S_{sat} - S_{res})[1 + (g_a|\psi|)^{g_n}]^{g_c} \quad (1)$$

where S_{res} is the residual saturation; $S_{sat} = 1$; g_a, $g_c = (1 - g_n)/g_n$ and g_n are fitting parameters (Table 3).

The relative permeability, k_{rel}, defined as the ratio of unsaturated and saturated soil permeabilities, is related to the effective saturation, $S_{eff} = (S - S_{res})/(S_{sat} - S_{res})$, and is calculated as:

$$k_{rel} = \max\left[S_{eff}^{g_l}\left(1 - \left[1 - S_{eff}^{\frac{g_n}{g_n-1}}\right]^{\frac{g_n-1}{g_n}}\right)^2 ; 10^4\right] \quad (2)$$

where g_l is a fitting parameter (Table 3).

3.1 Initial conditions

To model the initial hydraulic conditions of the slope, a constant hydraulic head was imposed at the left boundary, in a way that the calculated water table emerges at the average estimated value of 7 m depth at the top of the slope on the left-hand side. The average value has been chosen since the water table slightly varies (less than 1 m) during the seasons around a yearly average measured in the piezometric data. The hydraulic head is imposed on both the right-hand and left-hand sides (making the toe of the slope fully saturated), whereas a closed boundary is assumed at the bottom and seepage is possible on the surface.

A fully coupled analysis was run to get the initial hydro-mechanical conditions of the slope, without rain. Since the hydraulic conditions are an output of the coupled analysis, the results from the initial calculation steps are compared to average field measurements from boreholes 2 and 3 in terms of both PWP and S (calculated as the ratio between the measured VWC and the porosity of the materials measured in the lab) (Figure 3). Calculated PWP are in good agreement with measured average values in the shallowest layers, whereas the measurements in the deepest layer are overestimated (Figure 3(a)). This is probably due to the presence of a permeable layer below the marine clay, whose effect was disregarded for simplicity, resulting in a safe side estimation of PWP.

Calculated values of S were compared with both the yearly average measurements and the average measurements during fourteen days without rainfall (1-14 February 2017).

The comparison between the yearly average measurements and the measurements during the dry 14-days period (circles and crosses in Figure 3(b), respectively) shows that sensors below 2 m depth are slightly affected by external rainfall conditions. Furthermore, the calculated values before the application of rainfall are in good agreement with the measurements in dry conditions.

Table 2. Materials constitutive models and mechanical parameters in drained conditions.

Layer	Model	Unit weight (kN/m^3)	Young Modulus (MPa)	Poisson ratio (-)	Cohesion (kPa)	Friction angle (°)	Dilatancy (°)	Saturated permeability (m/d)	MCC param.: λ, κ, M (-)
Sandy silt	MC	18	15	0.3	0	36	8	0.2074	-
Silty sand	MC	18	15	0.3	0	32	8	8.6e-3	-
Clay	MCC	20	-	0.2	-	-	-	0.054e-3	0.058, 0.018, 1.2

Table 3. Van Genuchten parameters.

Layer	S_{res}	g_a	g_n	g_l
Sandy silt	0.067	1.689	1.9	-0.5884
Clayey silt	0.067	1.181	1.76	-0.5880
Clay	Fully saturated			

3.2 Rainfall scenarios

Since the measurements of PWP were not measured continuously since 2016, the numerical model was firstly tested using a rainfall sequence that occurred when data from all the sensors (PWP and VWC) were available for all the boreholes. This period coincides with rainfall and snowmelting data from 15 February to 15 March 2017 (Rainfall Event (RE) 1: Figure 4(a)). Secondly, the model (starting again from the initial conditions) was tested against a longer and more intense event that occurred in October 2019 (RE 2: Figure 4(b)).

Precipitation was applied vertically on the boundaries of the model that represent the ground surface. The infiltration was assumed to be coincident with the rainfall and snowmelt data (mm/d) reported in Figure 4.

On horizontal ground surfaces, the full precipitation (q) was applied. On a slope, with inclination α with respect to the horizontal, an infiltration perpendicular to the inclined boundary, with a magnitude of $q\cos\alpha$, was applied. To be on a safe side estimation of the slope deformations, potential run-off on the slope, as well as vegetation effects, were disregarded.

4 RESULTS AND DISCUSSION

Consistently with what happened in the real slope, none of the two rainfall events (REs) brought the slope to failure. In the analysis, the slope deformed at the end of both the REs with a maximum ground level horizontal displacement of about 4 cm at the toe of the slope and about 2 cm close to the railway line.

Figure 5 shows the results in terms of saturation profile against depth after the two considered REs. In particular, red lines are used in Figure 5(a) for the RE 1 and blue lines in Figure 5(b) for RE 2.

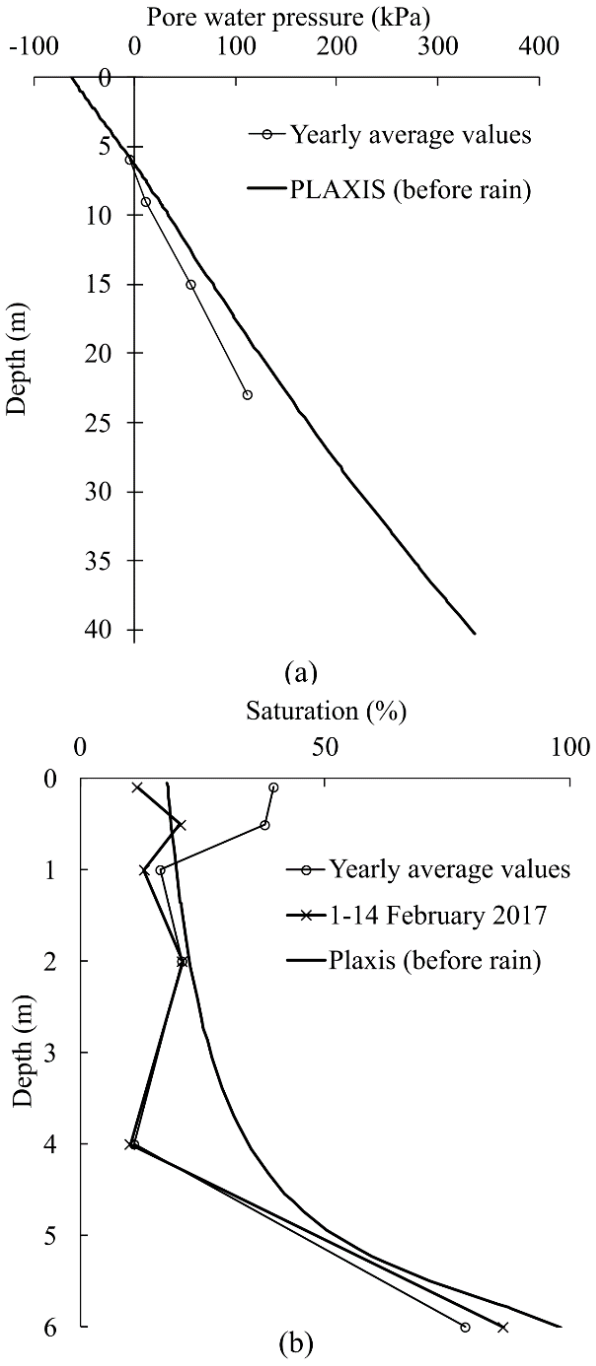

Figure 3 - Comparison between seasonal average values of field measurements and numerical results after the initial steps of the fully coupled analysis: (a) pore pressure in borehole 2 and (b) degree of saturation in borehole 3.

The results are compared against the measurements after the REs from VWC sensors in borehole 3. After both the REs, the calculated saturation slightly changes below 2 m depth ca (*i.e.* the numerical results before and after rain almost coincide). This means that the numerical model properly reproduces the internal infiltration flow previously observed from measurements in Figure 3.

The results close to the ground surface tend to overestimate the degree of saturation. This might be due, in reality, the slope is covered by vegetation, whose hydraulic effects are disregarded in the numerical model, for simplicity, e.g. decrease in soil permeability and delay of water infiltration, discussed in Rahardjo et al. (2014), Scholl et al. (2014) and Capobianco et al. (2021).

This assumption is likely to give a safe side estimation of the deformation of the slope. However, the numerical results close to the ground surface for RE 2 (Figure 5(b)) better approximate the measurements if compared to RE 1. This is because the hydraulic initial configuration of RE 2 is closer to the average initial configuration considered in this study, whereas RE 1 occurred after an unusual dry period.

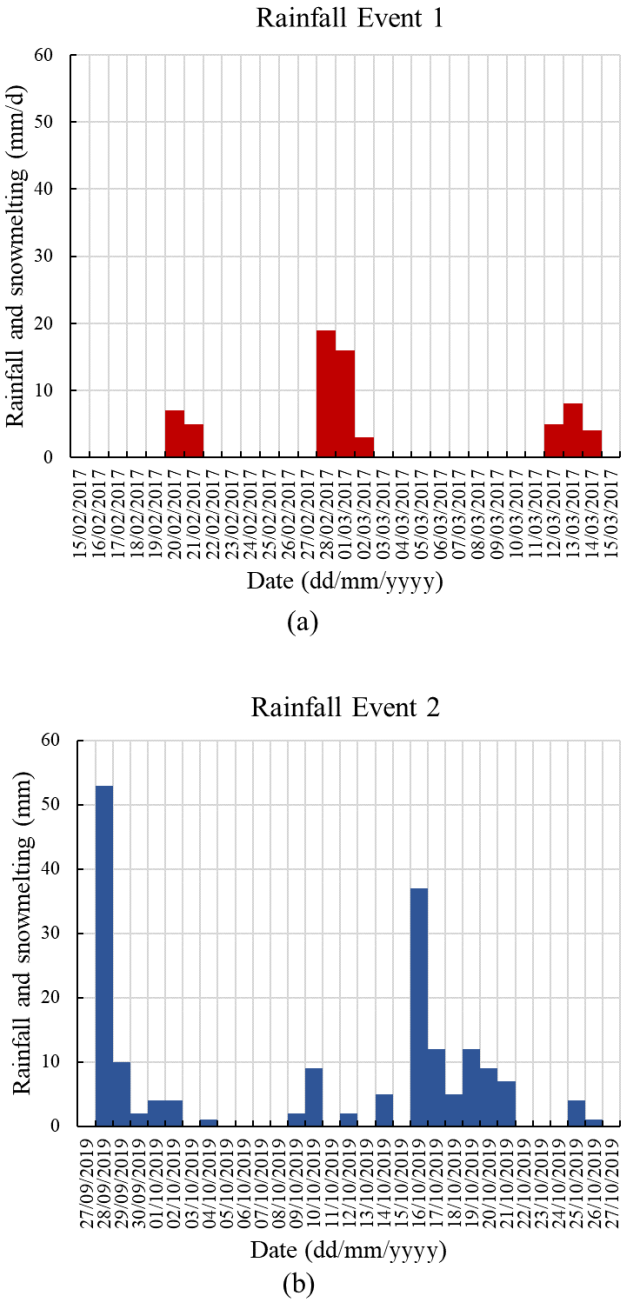

Figure 4 - Rainfall and snowmelting data series from Minnesund Station considered in this study. Measurements from (a) rainfall event 1 and (b) rainfall event 2.

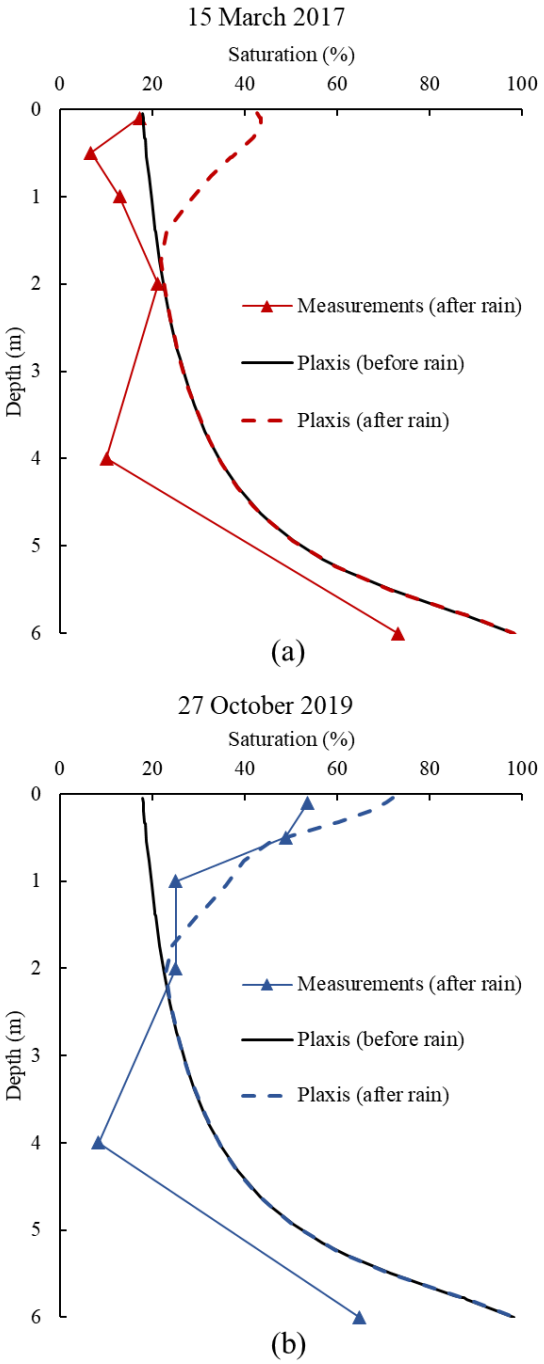

Figure 5 - Comparison between of data measured in borehole 3 and numerical results in terms of saturation after (a) RE 1 (March 15th 2017) and (b) RE 2 (October 27th 2019).

Despite the model giving safe-side estimation of potential instabilities, the fitting of numerical results with measurements might be improved by modelling the actual initial configuration of the water table instead of the average one.

Furthermore, the effects of vegetation might be included in the model.

5 CONCLUSIONS

In this study, an advanced finite element model was developed with the final goal of simulating the hydro-mechanical response of a Norwegian slope under two different rainfall scenarios. The mechanical properties of the materials and the initial conditions were calibrated against both field measurements and lab tests. The results were compared with available field data. The finite element model was able to capture some of the essential aspects of the infiltration mechanism due to precipitation through the slope surface, making it potentially suitable to be used as a tool to define triggering conditions of failure for future studies on the impact of climate change.

The procedure used in this study is completely general and based on simple principles of soil mechanics. It might be used for other similar applications where sufficient monitoring and site investigation data are available.

6 ACKNOWLEDGEMENTS

The authors acknowledge the financial support from Nordforsk (project #98335 NordicLink).

7 REFERENCES

Alonso, E.E., Gens, A., Delahaye, C.H. 2003. Influence of rainfall on the deformation and stability of a slope in overconsolidated clays: A case study. *Hydrogeol. J.* **11**.

BentleySystems, 2022. *Plaxis 2D Ultimate*; V22 (22.02.00.1078).

Capobianco, V., Cascini, L., Cuomo, S., Foresta, V. 2021. Wetting-drying response of an unsaturated pyroclastic soil vegetated with long-root grass. *Environ. Geotech.*

Heyerdahl, H., Høydal, Ø.A., Gisnås, K.G., Kvistedal, Y., Carotenuto, P. 2018. Slope instrumentation and unsaturated stability evaluation for steep natural slope close to railway line. In: *UNSAT 2018: The 7th International Conference on Unsaturated Soils*. pp. 1–6.

Piciullo, L., Capobianco, V., Heyerdahl, H. 2022. A first step towards a IoT-based local early warning system for an unsaturated slope in Norway. *Nat. Hazards* **114**, 3377–3407.

PLAXIS, 2021. *Scientific Manual*.

Rahardjo, H., Satyanaga, A., Leong, E.C., Santoso, V.A., Ng, Y.S. 2014. Performance of an instrumented slope covered with shrubs and deep-rooted grass. In: *Soils and Foundations*.

Salciarini, D., Tamagnini, C. 2015. *Physically – Based critical rainfall thresholds for unsaturated soil slopes.* Springer Ser. Geomech. Geoengin. 2015.

Scholl, P., Leitner, D., Kammerer, G., Loiskandl, W., Kaul, H.P., Bodner, G. 2014. Root induced changes of effective 1D hydraulic properties in a soil column. *Plant Soil* **381**.

van Genuchten, M.T. 1980. A Closed-form Equation for Predicting the Hydraulic Conductivity of Unsaturated Soils. *Soil Sci. Soc. Am. J.* **44**.